Is sea level rise accelerating in the Chesapeake Bay? A demonstration of a novel new approach for analyzing sea level data

Tal Ezer[1] and William Bryce Corlett[1,2]

Received 1 August 2012; revised 31 August 2012; accepted 1 September 2012; published 4 October 2012.

[1] Sea level data from the Chesapeake Bay are used to test a novel new analysis method for studies of sea level rise (SLR). The method, based on Empirical Mode Decomposition and Hilbert-Huang Transformation, separates the sea level trend from other oscillating modes and reveals how the mean sea level changes over time. Bootstrap calculations test the robustness of the method and provide confidence levels. The analysis shows that rates of SLR have increased from ~1–3 mm y^{-1} in the 1930s to ~4–10 mm y^{-1} in 2011, an acceleration of ~0.05–0.10 mm y^{-2} that is larger than most previous studies, but comparable to recent findings by Sallenger and collaborators. While land subsidence increases SLR rates in the bay relative to global SLR, the acceleration results support Sallenger et al.'s proposition that an additional contribution to SLR from climatic changes in ocean circulation is affecting the region. **Citation:** Ezer, T., and W. B. Corlett (2012), Is sea level rise accelerating in the Chesapeake Bay? A demonstration of a novel new approach for analyzing sea level data, *Geophys. Res. Lett.*, *39*, L19605, doi:10.1029/2012GL053435.

1. Introduction

[2] Communities along the shores of the Chesapeake Bay (CB), such as Norfolk, VA, have seen an increase frequency of flooding in recent years. Because of sea level rise (SLR), high tides or storm surges that caused little concern in the past, now result in a higher risk of flooding. Water level measurements in the CB in fact show that the relative sea level has been rising much faster than the globally mean absolute sea level trend. Past studies suggest that ~53% of the relative SLR in the region may be attributed to local land subsidence [*Boon et al.*, 2010, hereinafter BOO10]. However, the recent study by *Sallenger et al.* [2012, hereinafter SAL12], suggests a significant additional contribution to SLR from changes in ocean dynamics; SAL12 shows evidence for "hotspots" of accelerated SLR between Cape Hatteras and Cape Cod that may relate to warming of the sub-polar North Atlantic and slowing down of the Atlantic Meridional Overturning Circulation (AMOC). Note that the SLR acceleration rates reported by SAL12 are significantly higher than global acceleration rates reported by others [*Holgate*, 2007; *Church and White*, 2011; *Houston and Dean*, 2011]. Therefore, whether SLR is accelerating and by how much are highly contentious issues. Separating the SLR trend from decadal and multi-decadal oscillations is challenging. Local observations are also affected by spatial variations from local land subsidence, long-term post glacial rebound [*Tamisiea and Mitrovica*, 2011] and contributions from ocean dynamics [*Levermann et al.*, 2005; SAL12]. For example, along the North Atlantic coast, models [*Ezer*, 2001] and observations [*Sweet et al.*, 2009] found correlations between weakening of the Gulf Stream transport and increasing coastal sea levels; a result that can be explained by changes in sea level gradient across the Gulf Stream.

[3] Future projections and coastal risk assessments depend on whether SLR will continue at the same pace, at a reduced pace (i.e., SLR deceleration) or at a faster pace (i.e., SLR acceleration), so it is important to calculate SLR rates as accurately as possible and identify potential rate changes. However, the long-term sea level trend in tide gauge data is embedded in variations on many different time scales, from daily tides to the seasonal cycle, as well as interannual and decadal oceanic variations. Low-pass filters can remove seasonal and decadal variability and curve-fitting methods can be used to estimate trends, but the filtering may impact the calculated trend (BOO10). With these methods, at least 60-year record is needed for obtaining accuracy in SLR of ±0.5 mm y^{-1} with a 95% confidence level or obtaining accurate acceleration rates [*Douglas*, 2001; BOO10]. Standard curve fitting methods often show conflicting results even for long sea level records such as in Baltimore, MD (110 years) where *Houston and Dean* [2011] calculated a small deceleration of 0.003 mm y^{-2}, but SAL12 calculated acceleration of 0.044 mm y^{-2} since the 1950s; note however that in the lower Chesapeake Bay both Houston and Dean and SAL12 show positive SLR acceleration that agrees with our results. Those difficulties in calculating SLR trends and acceleration motivated this study, which will help future research in this field. The analysis method presented here can separate the trend from many oscillating modes, including long term cycles with periods longer than the record itself where only part of the cycle is captured by the data.

[4] The analysis method is based on Empirical Mode Decomposition, EMD, and Hilbert-Huang Transformation, HHT [*Huang et al.*, 1998], together with bootstrap simulations [*Mudelsee*, 2010]. The EMD/HHT method is especially useful for nonstationary and nonlinear time series, and has been used for different geophysical applications, such as earthquakes, hydrological and atmospheric data [*Rao and Hsu*, 2008] and oceanic internal waves [*Ezer et al.*, 2011]. The method decomposes any time series data into a finite number (~10) of intrinsic mode functions with time-variable amplitudes and frequencies. In most of the applications

[1]Center for Coastal Physical Oceanography, Old Dominion University, Norfolk, Virginia, USA.
[2]MSc Engineering in the Coastal Environment, University of Southampton, Southampton, UK.

Corresponding author: T. Ezer, Center for Coastal Physical Oceanography, Old Dominion University, 4111 Monarch Way, Norfolk, VA 23508, USA. (tezer@odu.edu)

0094-8276/12/2012GL053435

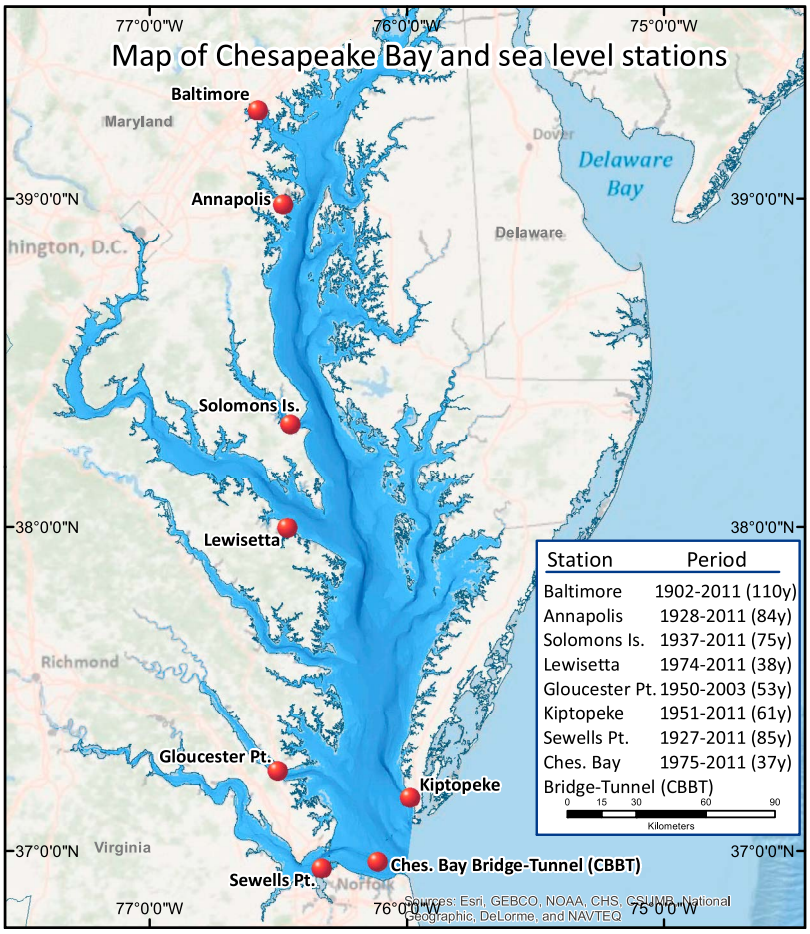

Figure 1. The location of the tide gauge stations (red circles) and the topography of the Chesapeake Bay (darker blue represents deeper waters). The period of measured sea level in each station is indicated in the inset.

mentioned above the method has been applied to study the EMD modes with high frequency. However, here a new (to our knowledge) application for sea level trend, using the method to separate oscillatory modes from the trend, is demonstrated. The calculated sea level trend can take any shape (i.e., the method is non-parametric) and there are no pre-determined cycles or time-scales that are removed (e.g., as in other filtering and harmonic methods), so one cannot predict ahead of time what shape the trend will take. If all stations show similar trend functions, it will indicate that they have been affected by the same process. Conversely, if the trends are very different from each other, it will indicate that local impacts from land motion, river flow or coastal dynamics are at play. Comparisons are made with results obtained from standard curve fitting methods.

[5] The paper is organized as follows. First, in section 2, the data and the analysis method are described, then in section 3, the results are presented, and finally, in section 4, discussions and conclusions are offered.

2. Method

[6] Monthly mean sea level records from 8 tide gauge stations in the CB were obtained from NOAA's "verified data" (http://tidesandcurrents.noaa.gov/). The stations are spread from the Chesapeake Bay Bridge Tunnel (CBBT) at the mouth of the bay to the city of Baltimore in the north (Figure 1). Record length ranges from 37 years (CBBT) to 110 years (Baltimore, MD). Most of these stations have been used in previous studies of SLR (e.g., BOO10 and SAL12).

[7] The analysis method is based on Empirical Mode Decomposition and Hilbert-Huang Transform [*Huang et al.*, 1998]; the EMD/HHT method is especially useful for applications that require time-series analysis of nonstationary records. A time series is decomposed into a finite number (∼10) of intrinsic oscillatory modes using the local maxima or minima envelop. The Hilbert Spectral analysis provides for each mode a time-dependent frequency and amplitude. Therefore, a time series of monthly sea level data at a particular station, $\eta(t)$, is decomposed into P modes of amplitude functions, $A^i(t)$, and frequency functions, $F^i(t)$, where i = 1, 2, .., P; the sum of all the modes reconstructs the original data, $\eta(t) = [A^1(t) + A^2(t) + \ldots A^P(t)]$. Each mode may represent different oceanic processes from the highest frequency (HHT mode 1) to the lowest frequency oscillating mode (HHT mode P-1). The remaining non-oscillating mode (HHT mode P) is the residual, i.e., $A^P(t)$, or the trend in the case of SLR. The analysis is demonstrated for the data in Sewells Point in Figure 2, where P = 9 (note that due to gaps in the early years, the analysis starts in 1948). Modes 1–3 (combined for clarity) represent annual to bi-annual variability, modes 4–8 represent 3–5 year interannual variations, modes 7–8 represent a multi-decadal ∼35-year cycle. Mode

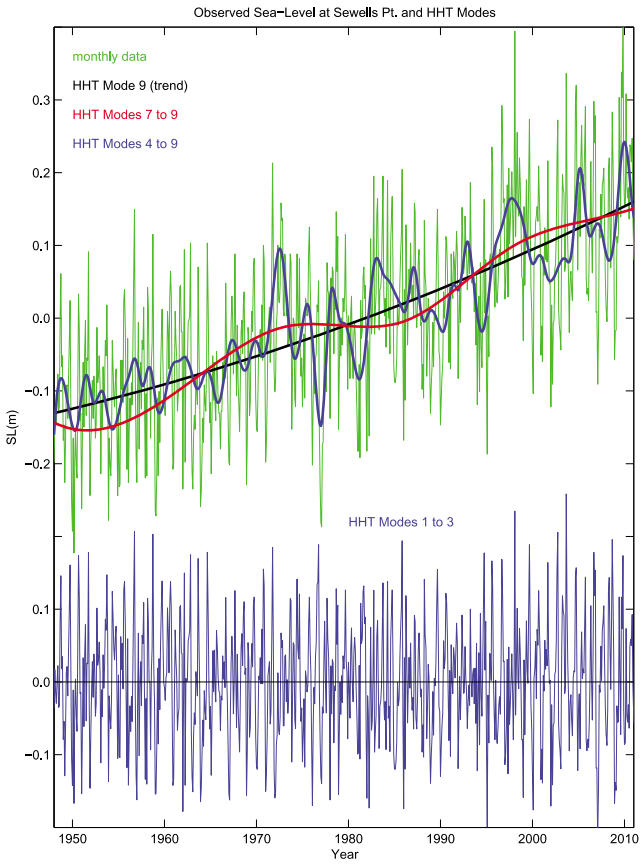

Figure 2. An example of the HHT analysis for the monthly sea level record at Sewells Point (thin green line). The observed record is decomposed into 9 modes, shown are the combined "high-frequency" modes 1 to 3 (thin blue line at the bottom), the "interannual-to-decadal" modes 4 to 9 (heavy blue line), the "multi-decadal" (~25 y period) modes 7 to 9 (heavy red line) and the remaining residual or "trend" mode 9 (heavy black line).

9 represents the remaining sea level trend. The focus of this study is on the trend (i.e., the last HHT mode), but it is clear that the analysis also provides a tool to study forcing mechanisms for other modes (which will be the focus of follow up studies).

[8] The HHT analysis is a more general filtering technique than fitting methods and thus the trend can take any monotonic shape that is not oscillating. Therefore, to demonstrate that the HHT method is useful for sea level studies we need to show that the method is robust within an acceptable statistical confidence level and that the trends are comparable with results obtained by other methods. The statistical confidence interval is calculated using a standard bootstrap method [*Mudelsee*, 2010]. The idea is to randomly resample the data many times in order to calculate error bars and confidence intervals. If a record includes M monthly data points, the sea level obtained from the HHT last mode P (i.e., the "trend") is $A^P(t)$ and the monthly anomaly relative to the trend is $\varepsilon(t)$,

$$A^P(t) = A^P_m = HHT(\eta_m); \tag{1a}$$

$$\varepsilon_m = \eta_m - A^P_m, \quad (m = 1,..,M). \tag{1b}$$

The bootstrap resampling approach is as follows. Step 1: an "artificial" sample sea level record is created by randomly sampling the anomalies from the original record,

$$\eta^*_m = A^P_m + \varepsilon_j, \qquad j = rand(1,\ldots,M). \tag{2}$$

Step 2: the HHT analysis is performed on the artificial data and an artificial trend is obtained,

$$A^{P*}_m = HHT\left(\eta^*_m\right), \quad (m = 1,..,M). \tag{3}$$

Step 3: the process (2)–(3) is repeated N times and then for each point m on the timeline the mean $\langle A^{P*}\rangle$ and the standard deviations s are calculated from all the artificial HHT results.

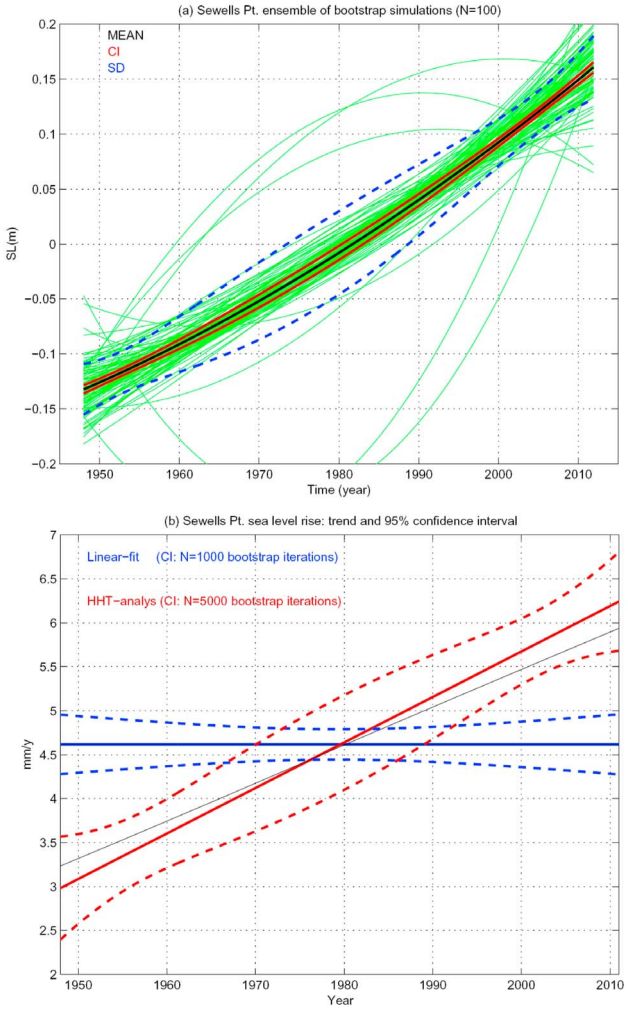

Figure 3. (a) An example of the bootstrap simulations of sea level at Sewells Point (last HHT mode) using N = 100 iterations; the green lines are individual simulations, the black line is the ensemble mean, the blue and red lines are the standard deviation and 95% CI, respectively. (b) SLR (in mm y^{-1}) from N = 5000 bootstrap iterations (mean is solid red and CI is dashed lines). The actual trend calculated from the real data (HHT mode 9 in Figure 2) is shown in thin black line. A bootstrap calculation for linear regression is shown in blue for N = 1000 iterations (the ensemble mean and the actual trend are indistinguishable for this case).

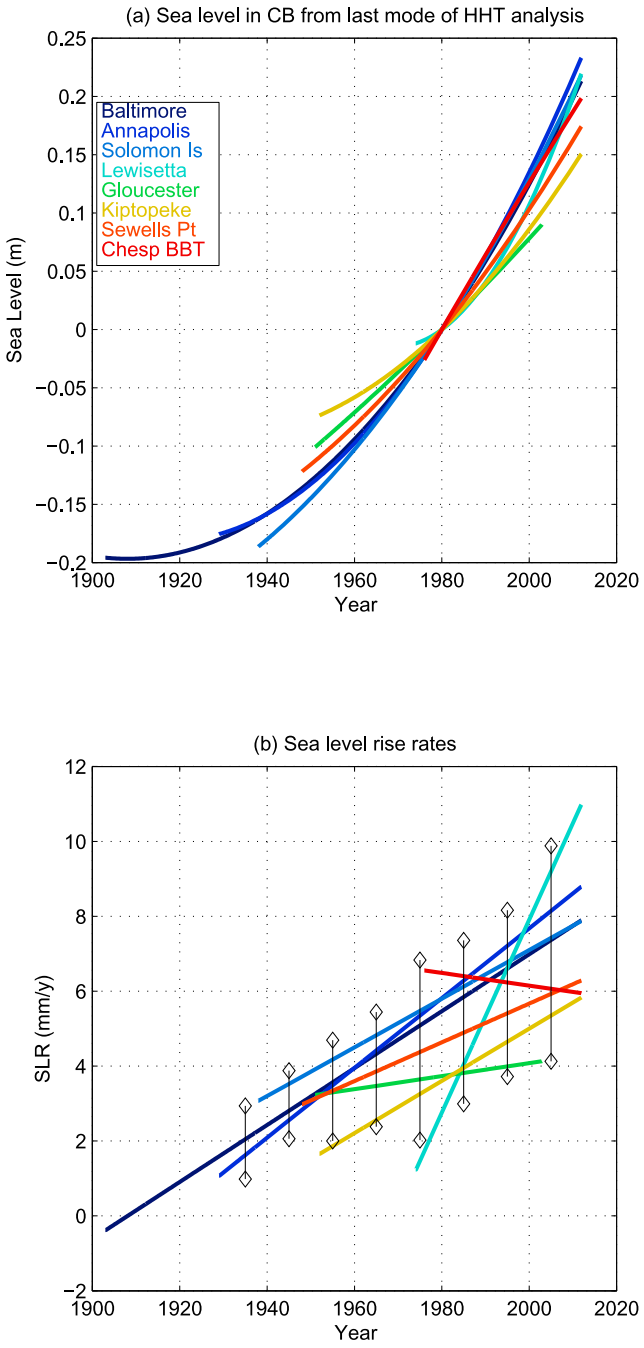

Figure 4. (a) The monthly sea level (in m) in the CB stations relative to the levels of 1980, as obtained from the last HHT mode. Colors in the blue to red range represent station locations from the upper to lower bay. (b) The SLR rates (in mm y^{-1}) calculated from the slope of the lines in Figure 4a. The vertical bars represent the range of ±2 standard deviations of the decadal means, from the 1930s to the 2000s.

The confidence interval around the mean can then be calculated [*Mudelsee*, 2010], using standard statistics such as Student-t distribution, t, for say 95% confidence level, $CI = [\langle A^{P*}\rangle - tsN^{-1/2}, \langle A^{P*}\rangle + tsN^{-1/2}]$. If the HHT analysis is robust, the mean $\langle A^{P*}\rangle$ will converge as the number of iterations increases and the actual trend A^P will be within the CI. Figure 3a demonstrates the bootstrap process for Sewells Point for $N = 100$ iterations. The green lines are the individual simulations of equation (3), the black line is the mean $\langle A^{P*}\rangle$ and the range of s and CI are shown in blue and red, respectively. The SLR rate can be calculated from the slope of the mean in Figure 3a and is shown in Figure 3b (red solid line). To achieve a mean SLR rate that is statistically significant at 95% confidence within ±0.5 mm y^{-1}, requires about $N = 5000$ simulations (Figure 3b). The results show almost a steady increase in SLR, i.e., a constant positive acceleration. The SLR calculated from the real data (black line in Figure 3b), has slightly smaller acceleration than the mean, but within the 95% CI lines, indicating that the method is statistically sound given the observed variability. Similar bootstrap calculations with a linear regression fitting for the same data (blue lines in Figure 3b), requires less than 1000 simulations to achieve the same CI; the linear regression represents the mean SLR rate. The CI of the HHT analysis

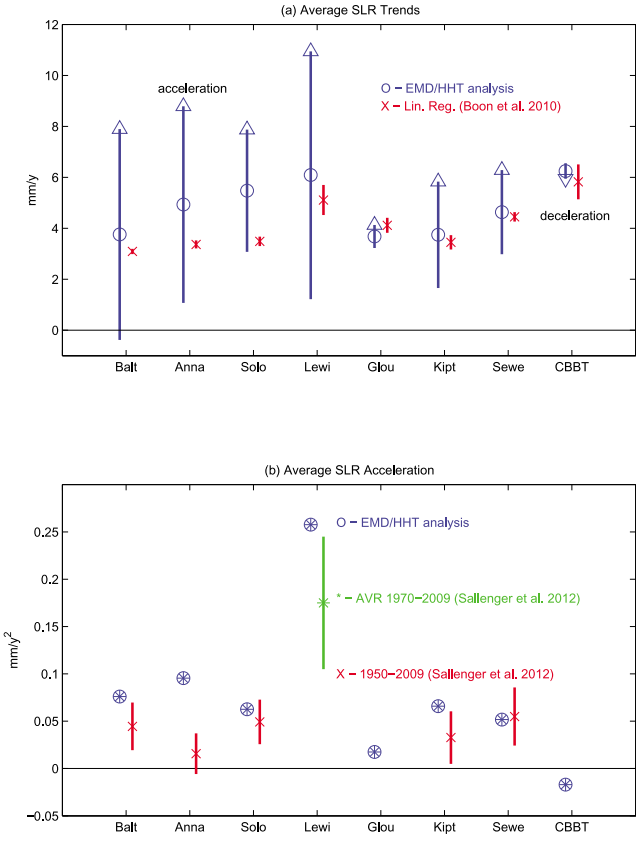

Figure 5. (a) Comparison between the SLR average rates (blue circles) and change of rates (blue lines with up/down arrows indicating acceleration/deceleration trends) obtained from the HHT analysis and the average rates and 99% CI (in red) obtained from a linear regression by BOO10. (b) Comparison between the SLR average acceleration obtained from the HHT analysis (blue) and the mean acceleration and variability (±2 standard deviations) calculated from a 60-year (1950–2009) quadratic regression fitting by SAL12 (red "X" and lines). The HHT acceleration in Lewisetta (1974–2011) is compared with the average acceleration for 1970–2009, as calculated for the "hotspots" by SAL12 (green).

indicates that SLR rates before 1970 are statistically different than the SLR rates after 1990.

3. Results

[11] Figure 4a summarizes the changes of sea level in the 8 CB stations, as obtained from the last HHT mode of each station; these changes represent the instantaneous mean sea level after all the oscillatory modes are removed. Qualitatively, it is clear that the sea level is rising faster now than in the past, this is especially apparent in the long records such as those in Baltimore and Annapolis. The change in sea level over the past ~30 years, from 1980 to 2011, is almost the same for 5 out of 8 stations (Baltimore, Annapolis, Solomon Island, Lewisetta and CBBT), however, in two stations the changes in sea level are somewhat different than in other stations (Figure 4b). At CBBT the current SLR rate is high, but the rate seems to be almost constant with slight decrease over the past 30 years, while at Lewisetta the SLR seems to increase much faster than at any other location. The records in these two stations are less than half the length of the other stations, so the calculations are less accurate. However, there is also the possibility that SLR rates have changed significantly in recent decades (SAL12). Gloucester Point and Kiptopeke are located at similar latitudes across the CB (Figure 1) and have different SLR pattern (Figure 4b), which suggests possible differences in local land subsidence. The analysis indicates recent SLR rates of ~6 mm y^{-1} in the lower bay (CBBT, Sewells Point and Kiptopeke) and ~8 mm y^{-1} in the upper bay (Baltimore, Annapolis and Solomon Island), and bay-wide rate changed from ~1–3 mm y^{-1} in the 1930s to ~4–10 mm y^{-1} in 2011 (within 2 standard deviations).

[12] The EMD/HHT results are compared with SLR rates obtained from linear regression by BOO10 (Figure 5a) and SLR acceleration rates obtained from quadratic regression by SAL12 (Figure 5b). The SLR trends show acceleration for all the stations except CBBT; the CBBT record at the mouth of the CB is relatively short and the tide gauge is located on a man-made island to support bridge infrastructure, so land subsidence and ocean dynamics there are expected to be different than coastal stations. Both, our analysis and BOO10's show similar spatial variations, with increasing mean SLR rates from the upper bay at Baltimore southward to Lewisetta, a drop in rates, and then another increase from Kiptopeke to CBBT (Figure 5a). The mean acceleration obtained from the HHT analysis (blue circles in Figure 5b) is simply the average slope of each line in Figure 4b; the latter is the slope of the last HHT mode in Figure 4a. SAL12 calculated acceleration rates from a quadratic regression for 40-year records (1970–2009), for 50-year records (1960–2009), and for 60-year records (1950–2009), and they found considerably larger acceleration in 1970–2009 than in 1950–2009 (SAL12, supplementary Figure S4). Four stations (Baltimore, Solomon Island, Kiptopeke and Sewells Point) had results similar to SAL12's, but the Annapolis results show significantly higher acceleration (0.095 mm y^{-2}) than SAL12's (0.016 mm y^{-2}); in our calculations Annapolis is more similar to nearby Baltimore, both in trend (Figure 5a) and acceleration (Figure 5b). The acceleration at Lewisetta (0.257 mm y^{-2}) is unusually higher than any other station (see also Figure 4b); this station has a relatively short record starting in 1974 so it was not included in SAL12's analysis. However, acceleration in Lewisetta is better compared with the average acceleration calculated by SAL12 for 1970–2009, ~0.1–0.25 mm y^{-2} (green line in Figure 5b).

4. Summary and Conclusions

[13] A new method to analyze sea level data and calculate instantaneous SLR rates and accelerations is introduced. The method is demonstrated for sea level data from the Chesapeake Bay, an area of increasing risk of coastal flooding due to high SLR. Standard methods often filter a few selected oscillations such as the seasonal cycle (which is well known) or decadal variability (mostly unknown), and then calculate SLR trends by linear regression or SLR acceleration by quadratic fitting. The proposed EMD/HHT method [*Huang et al.*, 1998] extracts a trend from noisy data by systematically filtering out up to ~10 oscillating non-stationary modes, including low frequency modes with periods as long as twice the record length (which is not possible with standard spectral and harmonic methods). The hypothesis behind our study is that the remaining non-oscillating last HHT mode represents the mean sea level trend. Note that the oscillating modes that are removed here (Figure 2) are also a useful product to study seasonal, interannual and decadal variability (they will be discussed in separate studies). Bootstrap calculations show that the method is robust and statistically sound.

[14] Our results are consistent with SLR rates calculated by BOO10 and the recent SLR acceleration rates calculated by SAL12, and show a statistically significant increase in SLR rates from ~1–3 mm y^{-1} in the 1930s to ~4–10 mm y^{-1} in the last decade. The spatial pattern of SLR rates within the CB may relate to land subsidence (BOO10), but since post-glacial subsidence has a very long time scales it does not affect SLR acceleration (SAL12), so the similar acceleration found here in 5 of 8 records supports SAL12's hypothesis that climatic changes in the North Atlantic circulation may impact the region's sea level. The calculated acceleration rates of ~0.05–0.1 mm y^{-2} in most of the CB stations are larger than previous global estimates [*Church and White*, 2011; *Holgate*, 2007; *Houston and Dean*, 2011], but are very similar to the high-acceleration "hotspots" in the North Atlantic coast (SAL12). The main purpose of this study was to introduce and test the new analysis tool. Together with other methods it will help to better understand the processes affecting coastal SLR such as the impact from ocean dynamics and from subsidence, and also will help to improve future projections of SLR and coastal risk assessments.

[15] **Acknowledgments.** ODU's Climate Change and Sea Level Rise Initiative (CCSLRI) and its director, L. Atkinson, as well the Center for Coastal Physical Oceanography (CCPO) and its director J. Klinck, provided motivation, advice and partial support for this study. C. Grosch suggested the bootstrap calculations and G. McLeod helped with some figures. K. Doran and A. Sallenger provided us with their data. Co-author W. B. Corlett recently received a BA in oceanography and coastal engineering from ODU and was supported by various scholarships for his undergraduate research. T. Ezer is partly supported by grants from NOAA.

[16] The Editor thanks the two anonymous reviewers for their assistance in evaluating this paper.

References

Boon, J. D., J. M. Brubaker, and D. R. Forrest (2010), Chesapeake Bay land subsidence and sea level change, in *Applied Marine Science and Ocean Engineering*, *Rep. 425*, pp. 1–41, Va. Inst. of Mar. Sci., Gloucester Point.

Church, J. A., and N. J. White (2011), Sea-level rise from the late 19th to the early 21st century, *Surv. Geophys.*, *32*, 585–602, doi:10.1007/s10712-011-9119-1.

Douglas, B. C. (2001), Sea level change in the era of the recording tide gauge, in *Sea Level Rise: History and Consequences*, *Int. Geophys. Ser.*, vol. 75, edited by B. C. Douglas, M. S. Kearney, and S. P. Leatherman, chap. 3, pp. 37–64, Elsevier, New York.

Ezer, T. (2001), Can long-term variability in the Gulf Stream transport be inferred from sea level?, *Geophys. Res. Lett.*, *28*(6), 1031–1034, doi:10.1029/2000GL011640.

Ezer, T., W. D. Heyman, C. Houser, and B. Kjerfve (2011), Modeling and observations of high-frequency flow variability and internal waves at a Caribbean reef spawning aggregation site, *Ocean Dyn.*, *61*(5), 581–598, doi:10.1007/s10236-010-0367-2.

Holgate, S. J. (2007), On the decadal rates of sea level change during the twentieth century, *Geophys. Res. Lett.*, *34*, L01602, doi:10.1029/2006GL028492.

Houston, J. R., and R. G. Dean (2011), Sea-level acceleration based on U.S. tide gauges and extensions of previous global-gauge analyses, *J. Coastal Res.*, *27*(3), 409–417, doi:10.2112/JCOASTRES-D-10-00157.1.

Huang, N. E., Z. Shen, S. R. Long, M. C. Wu, E. H. Shih, Q. Zheng, C. C. Tung, and H. H. Liu (1998), The empirical mode decomposition and the Hilbert spectrum for non stationary time series analysis, *Proc. R. Soc. London*, *454*, 903–995, doi:10.1098/rspa.1998.0193.

Levermann, A., A. Griesel, M. Hofmann, M. Montoya, and S. Rahmstorf (2005), Dynamic sea level changes following changes in the thermohaline circulation, *Clim. Dyn.*, *24*(4), 347–354, doi:10.1007/s00382-004-0505-y.

Mudelsee, M. (2010), *Climate Time Series Analysis: Classical Statistical and Bootstrap Methods*, 474 pp., Springer, Dordrecht, Netherlands.

Rao, A. R., and E.-C. Hsu (2008), *Hilbert-Huang Transform Analysis of Hydrological and Environmental Time Series*, *Water Sci. Technol. Libr.*, vol. 60, 248 pp., Springer, Dordrecht, Netherlands.

Sallenger, A. H., K. S. Doran, and P. Howd (2012), Hotspot of accelerated sea-level rise on the Atlantic coast of North America, *Nature, Clim. Change*, doi:10.1038/nclimate1597, in press.

Sweet, W., C. Zervas, and S. Gill (2009), Elevated east coast sea level anomaly: June–July 2009, *NOAA Tech. Rep. NOS CO-OPS 051*, 40 pp., Natl. Ocean Serv., Silver Spring, Md.

Tamisiea, M. E., and J. X. Mitrovica (2011), The moving boundaries of sea level change, *Oceanography*, *24*(2), 24–39, doi:10.5670/oceanog.2011.25.